JOURNAL OF Materials CHEMISTRY

Cobalt–iron hydroxycarbonates and their evolution to mixed oxides with spinel structure

Margarita del Arco, Raquel Trujillano and Vicente Rives*

Departamento de Química Inorgánica, Universidad de Salamanca, Salamanca, Spain

Cobalt(II)–iron(III) mixed hydroxides with hydrotalcite-like structure have been synthesized. Depending on the experimental conditions during synthesis, Co^{II} becomes partially oxidized to Co^{III}. The solids have been characterized by X-ray diffraction, FTIR spectroscopy, temperature-programmed reduction and nitrogen adsorption at low temperature for specific surface area assessment. Reduction of Fe^{III} takes place at lower temperatures than that of bulk Fe_3O_4. Thermal treatment in air leads to oxidation of Co^{II} to Co^{III}, in the same temperature range where collapsing of the layered structure by decarbonation is observed. The nature of the spinel phases formed upon calcination at high temperature depends both on the calcination temperature and the calcination time.

Transition metals belonging to groups 8–10 and their alloys, as well as their oxides, are widely used as catalysts, both as bulk materials or supported on other oxides. These catalysts can be prepared following different routes.[1] The use of multicomponent catalysts is however limited because of a lack in the structural homogeneity and/or chemical segregation, that generally lead to lower catalytic activity and changes in selectivity. An alternative to overcome this problem is to use different precursors, and the so-called 'anionic clays' seem to be good precursors to prepare these catalysts. Among these anionic clays, the most widely used systems have the hydrotalcite structure, and so they are usually known as 'hydrotalcite-like' compounds (HT). These are layered double hydroxides with the general formula $[M^{II}_{1-x}M^{III}_{x}(OH)_2]^{x+}(X)_{x/m}\cdot nH_2O$ [M^{II} = Mg, Zn, Ni, *etc.* M^{III} = Al, Fe, Cr, *etc.* X = anion (carbonate, sulfate, nitrate, chloride, *etc.*)]. The structure consists of brucite layers which are positively charged because of partial substitution by trivalent cations, with the interlayer space filled with anions (to balance the positive charge of the layers) and water molecules. The same structure is also shown by compounds containing monovalent–trivalent cations (Li, Al) and even divalent–tetravalent (Co, Ti) cations. These materials exhibit anion-exchange properties and their properties have been recently reviewed.[2–4] Upon thermal decomposition they lead to mixed oxides,[2,5,6] and, depending on the nature of the cations and the calcination temperature, recovering of the layered structure upon rehydration of these mixed oxides is possible.[7]

Here, we report on the synthesis and thermal properties of layered double hydroxides with the hydrotalcite structure containing Co^{II} and Fe^{III} as layer cations, prepared by coprecipitation. Hansen *et al.* have recently reported[8] the synthesis of these materials; in our case, the use of different experimental conditions during synthesis has led to partial oxidation of Co^{II} to Co^{III}. The cobaltites obtained by thermal decomposition are currently being studied as total oxidation catalysts.

Experimental

All reagents used were from Fluka (Germany). A solution containing 0.12 mol $Co(NO_3)_2\cdot 6H_2O$ and 0.06 mol $Fe(NO_3)_3\cdot 9H_2O$ in 250 ml double-distilled water was dropwise added (*ca.* 30 drops min^{-1}) to a solution containing 0.31 mol Na_2CO_3 in 500 ml double-distilled water. The mixture was vigorously stirred and maintained at *ca.* 330 K for 30 h. The suspension showed a pale brown colour. Two portions of the suspension were submitted to the following treatments: (i) washing until total removal of NO_3^- and Na^+,[9] filtering and drying in air at 343 K; this sample is denoted CoFeI; (ii) hydrothermal treatment at 370 K over 5 days in a stainless steel digestion bomb lined with Teflon; the solid was washed until total removal of NO_3^- and Na^+, filtered and dried at room temperature in open air, leading to sample CoFeH. In order to avoid partial oxidation of Co^{II} species to Co^{III}, presumably taking places during these treatments and already reported for other Co-containing hydrotalcites,[10,11] a third sample, denoted CoFeII, was prepared similarly to sample CoFeI, but in this case the solid was dried in open air at room temperature. For reasons given below, the solids were then calcined in air at 623 or 1023 K.

Chemical analysis for cobalt and iron were carried out by atomic absorption in a Mark-II ELL-240 instrument. Powder X-ray diffraction (PXRD) diagrams were recorded in a Siemens D-500 apparatus, using Cu-Kα radiation, connected to a DACO-MP microprocessor with Diffract/AT software. Differential thermal analyses (DTA) and thermogravimetry (TG) were recorded in air or in nitrogen in DTA-1700 and TGS-2 instruments, respectively, from Perkin-Elmer, connected to a Perkin-Elmer 3600 data station, at a heating rate of 10 K min^{-1}. The FTIR spectra were recorded in a FTIR 1730 Perkin Elmer instrument using the KBr pellet technique; one hundred scans were averaged, with a nominal resolution of 4 cm^{-1}. Specific surface area and porosity assessment was carried out from the nitrogen adsorption isotherms at 77 K, measured in a conventional high vacuum system, provided with a silicon oil diffusion pump, McLeod gauge, grease-free stopcocks and a Baratron MKS pressure transducer; analysis of the isotherms was performed with the assistance of a computer program described elsewhere.[12] Temperature-programmed reduction (TPR) analyses were carried out in a Micromeritics TPR/TPD 2900 instrument, at a heating rate of 10 K min^{-1}, and using *ca.* 10 mg of sample and a H_2–Ar (5 vol%) mixture (from Sociedad Española del Oxígeno, Spain) as reducing agent (60 ml min^{-1}); experimental conditions for TPR runs were chosen according to data reported elsewhere[13] in order to attain good resolution of component peaks; calibration was carried out from reduction of CuO (from Merck).

Results and Discussion

Chemical analysis and X-ray diffraction

Results for chemical analysis (metals) of the samples are given in Table 1. The Co/Fe (corresponding to the M^{II}/M^{III} atomic

Table 1 Chemical composition (metals), chemical formulae and lattice parameters for the starting samples

sample	Co[a]	Fe[a]	Co/Fe[b]	formula[c]	c/Å	a/Å
CoFeI	39.0	14.2	2.72	$[Co_{0.70}Fe_{0.30}(OH)_2](CO_3)_{0.150}\cdot 0.18H_2O$	22.7	3.11
CoFeH	40.5	15.8	2.34	$[Co_{0.73}Fe_{0.27}(OH)_2](CO_3)_{0.135}\cdot 0.04H_2O$	22.8	3.12
CoFeII	34.9	13.8	2.40	$[Co_{0.71}Fe_{0.29}(OH)_2](CO_3)_{0.145}\cdot 0.94H_2O$	22.7	3.12

[a]Mass%. [b]Atomic ratio. [c]Rounded value assuming 2 OH.

ratio in the hydrotalcite, if no oxidation of Co^{II} to Co^{III} takes place) is almost the same in both samples not submitted to hydrothermal treatment, despite the fact that they were prepared by different procedures. It should be noted that reproducibility of the atomic ratio values in hydrotalcites prepared in different processes is rarely achieved. The similar Co/Fe ratio in both samples is, however, compatible with the lower Co and Fe contents in sample CoFeII if it is taken into account that water is present in the samples and that sample CoFeII which was dried at room temperature, would be expected to have a larger water content. In sample CoFeH the Co/Fe ratio is slightly lower, thus indicating a larger Co/Fe substitution in the brucite-like layers. If all cobalt is assumed to be Co^{II}, these values are within the range where a true anionic clay structure should be formed, according to data reported elsewhere.[2,4]

Assuming no Co^{II} oxidation to Co^{III} in any of the samples, the chemical formulae in Table 1 can be calculated; the water content has been calculated from TG analysis (see below).

Similar powder X-ray diffraction diagrams were recorded for the three samples, Fig. 1. The peaks correspond to a hydrotalcite-like structure. The difference in the sharpness of the peaks is a result of the different treatments to which the samples have been submitted; hydrothermal treatment leads to an increase in the particle size,[14] and the corresponding diffraction peaks are sharper and more intense, as observed here for sample CoFeH. Basal plane diffractions correspond to planes (003), (006), (009) if a rhombohedral symmetry (3R) is assumed for the crystal.[15,16] These diffractions are recorded at *ca.* 7.58, 3.79 and 2.54 Å, very close to those reported in the literature[2] for hydrotalcite-like materials containing interlayer carbonate anions. The thickness of the brucite-like layer is almost constant for most hydrotalcites synthesized of first series transition cations, as it mainly depends on the ionic radii of the cations existing in the layers and of the hydroxy group, and so basal plane spacings depend mostly on the nature and orientation of interlayer anions.[2,3,17,18] Parameter c of the crystal corresponds to $c=3\times d(003)$, while parameter a, corresponding to cation–cation distances within the brucite-like layer, can be calculated as $a=2\times d(110)$, the peak corresponding to planes (110) being the first of the doublet recorded at 2θ *ca.* 55–60° (Cu-Kα). The values calculated for the three samples are given in Table 1. Overall, the sharpness of the peaks (tentatively taken as an indication of the crystallinity of the samples) increases in the order CoFeII < CoFeI < CoFeH, *i.e.*, the more severe the thermal treatment during synthesis, the sharper the PXRD peaks recorded.

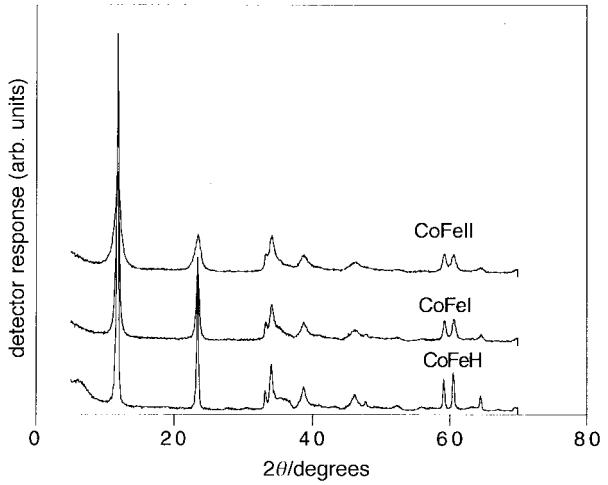

Fig. 1 Powder X-ray diffraction patterns of samples CoFeI, CoFeH and CoFeII

FTIR spectroscopy

The positions of the recorded bands, as well as their assignments, are given in Table 2. The band around 3400 cm^{-1}, recorded in all samples, is due to the hydroxy stretching mode, and is very broad owing to the presence of variable strength hydrogen bonds in the structure, among the interlayer water molecules, and among these and the layer hydroxy groups. The shoulder at *ca.* 3050 cm^{-1} has been ascribed[19,20] to the stretching mode of hydroxy groups hydrogen-bonded to interlayer carbonate anions. The medium intensity band at 1600–1640 cm^{-1} is due to the bending mode of interlayer molecular water molecules. The most intense band is recorded at *ca.* 1350 cm^{-1}, and corresponds to mode v_3 of interlayer carbonate anions. Although this position is quite apart from that corresponding to free carbonate,[21] the restricted symmetry in the interlayer space of the hydrotalcite would account for this apparently abnormal behaviour. Also this restricted symmetry would be responsible for activation of mode v_1, IR forbidden for pure D_{3h} symmetry. Other bands at lower wavenumbers are due to M—O and M—O—M vibration modes.

Surface texture

The surface texture properties of the samples have been assessed from nitrogen adsorption isotherms at 77 K. These correspond to type II in the IUPAC classification,[22] indicating the absence of micropores. Those for samples CoFeI and CoFeII show a hysteresis loop closing at $P/P_0=0.3$–0.5, while for sample CoFeH the isotherm is completely reversible.

The specific surface area values, as determined by the BET method, were 178, 42 and 77 $m^2\ g^{-1}$ for samples CoFeI, CoFeH and CoFeII, respectively. The adsorption capacity for sample CoFeH is much lower than for sample CoFeI, and thus the specific surface area values change accordingly. The absence of micropores is also concluded from the V–t plots, consisting of straight lines passing through the origin. The pore size distribution analysis indicates a major contribution by pores with an average diameter of *ca.* 2.5 nm, but in sample CoFeI a contribution by pores with an average diameter of 5 nm and higher is also observed.

Thermal properties: differential thermal analysis and thermogravimetry

Owing to the presence of oxidizable Co^{II} cations, these analyses were carried out both in air and in nitrogen. The curves obtained are shown in Fig. 2.

The TG curves are very similar in all cases, with a single mass loss. Other hydrotalcites show two mass losses,[14,23] but usually they merge into a single step in systems containing transition metal cations.[11,24–26] These steps are due to (i) dehydration (removal of water molecules from the interlayer space) and to (ii) dehydroxylation (removal of water molecules

Table 2 Positions (cm^{-1}) and assignment of the bands recorded in the FTIR spectra of the samples

assignment	CoFeI	CoFeH	CoFeII	ref. 6	ref. 8
ν(OH)	3400	3400	3420	3450	3446
	3049(sh)[a]	3049(sh)			3010
$\delta(H_2O)$	1645	1635	1637	1630	1632
$\nu_3(CO_3^{2-})$	1358	1358	1352	1352	1354
$\nu_1(CO_3^{2-})$	1060	1060	1060	1070	
$\nu_2(CO_3^{2-})$	840(sh)	840(sh)	840(sh)	840(sh)	840(sh)
ν(M—OH)	780	780	773	760	760(sh)
$\nu_4(CO_3^{2-})$		644	639		624(sh)
other bands	532	532			
			502		516
	488(sh)	488(sh)			489

[a]sh = shoulder.

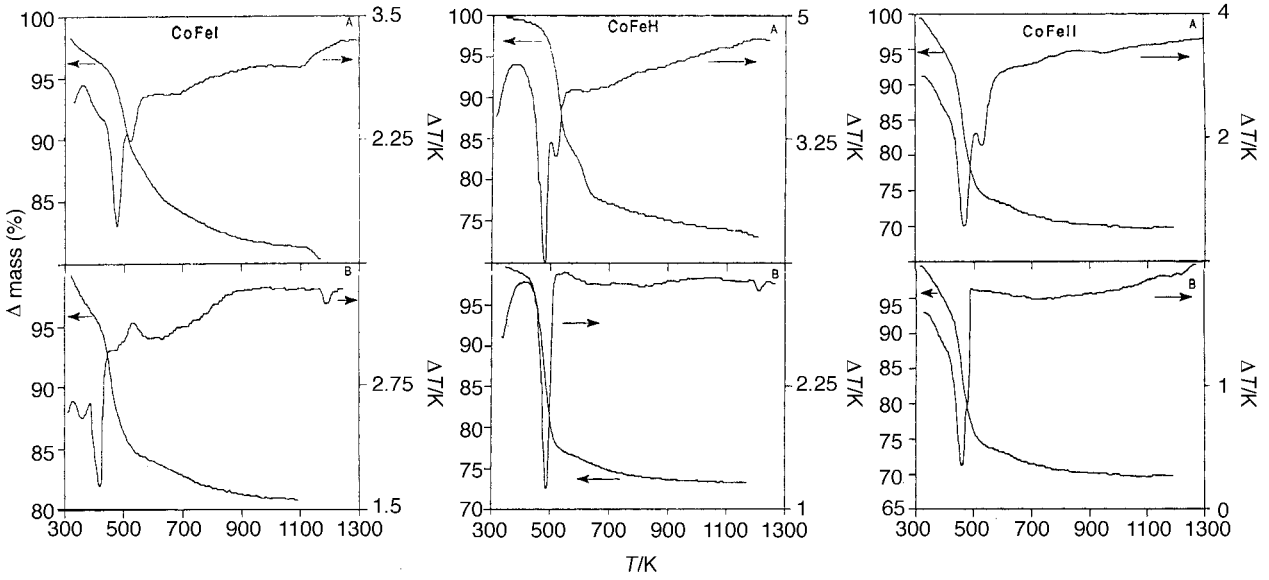

Fig. 2 DTA–TG curves for samples CoFeI, CoFeH and CoFeII, recorded in (A) nitrogen and (B) air

through condensation of brucite-layer hydroxy groups) and decarbonation (from interlayer carbonate anions).

Mass loss starts from the start of the analysis for samples CoFeI and CoFeII, while for sample CoFeH mass loss starts at *ca.* 450 K. This behaviour is undoubtedly related to the hydrothermal treatment of this sample, while the mass loss at low temperature for the other two samples should correspond to removal of physisorbed water, because of their large specific surface areas.

The DTA curves show two endothermic effects below 600 K when the analyses are performed in nitrogen, but a single peak when the curve is recorded in air. Also, the high-temperature side of the main endothermic peak is almost vertical in the curves corresponding to the analyses performed in air. It is also worth noting that the main difference seems to be that the endothermic peak recorded in air for sample CoFeI is *ca.* 60 K below that for the other samples. In this case, in addition, a weak exothermic effect is noted at *ca.* 600 K.

Some of us[10] have previously described a similar behaviour for Co,Al-carbonate hydrotalcites; air gives rise to the (at least partial) oxidation of Co^{II} to Co^{III}, an exothermic process, taking place in the same temperature range corresponding to the second exothermic effect recorded in nitrogen. Thus, both effects (endothermic, for carbonate and hydroxy removal, and exothermic, for Co^{II} oxidation) would cancel each other to some extent in the DTA curve. Klissurski and co-workers[6] have also claimed that the exothermic effect is very weak when the analysis is performed in air, since Co^{II} oxidation occurs simultaneously with thermolysis of the solids. Porta *et al.*[27] have reported that Cu,Co hydrotalcites decompose in a single step both in nitrogen and in air, although decomposition in nitrogen takes place *ca.* 60 K above decomposition in air, and ascribe this difference to the nature of the oxides formed, CoO ($\Delta G^\circ_f = -214$ kJ mol Co^{-1}) in nitrogen, but Co_3O_4 ($\Delta G^\circ_f = -258$ kJ mol Co^{-1}) in air. For our sample, CoFeI, as the main endothermic effect is recorded at a lower temperature than in the other two samples, the exothermic effect is clearly recorded in air at *ca.* 600 K. The weak endothermic effect recorded at high temperature in air for samples CoFeI and CoFeH should correspond to decomposition of Co_3O_4 (presumably formed during decomposition), in a similar way to that reported by Porta *et al.*,[27] to rock-salt structure CoO.[6,28]

Temperature-programmed reduction

Analysis of the reducibility of the samples by TPR has been used in order to monitor oxidation of cobalt during preparation of the samples. Partial oxidation of Co^{II} to Co^{III} in Co,Al hydrotalcite-like compounds has been previously reported,[10] and strongly depends on the experimental conditions during preparation of the samples. The technique has proved to be valuable for characterization of layered double hydroxides with oxidizable/reducible cations.[29] In order to analyze the reduction of the cations existing in our samples, reduction of reference materials has been previously studied.

Well crystallized Co_3O_4 reduces in two steps, with maxima at 549 ± 5 and 610 ± 5 K, respectively, the exact positions of the peaks depending on the degree of crystallization. The relative intensities of these two peaks, however, remain the same, 1:3, with a (total H_2)/Co ratio of *ca.* 1.30 (expected

value for total reduction to Co^0 1.33). Taking into account the ratio between the areas of both component peaks, a two-step reduction process can be assumed:

$$Co_3O_4 + H_2 \rightarrow 3\ CoO + H_2O \quad (1)$$

$$3\ CoO + 3\ H_2 \rightarrow 3\ Co + 3\ H_2O \quad (2)$$

i.e., under these experimental conditions, Co_3O_4 is reduced to the metallic state, probably through intermediate formation of CoO.

Reduction of Fe_2O_3 has been previously analyzed by DTA and TG.[30] In our experimental system, reduction of Fe_2O_3 previously calcined at *ca.* 1000 K gives rise to a less clear profile than that recorded for Co_3O_4. After a weak peak at 670 K, a broad feature centered at 800 K is recorded, reduction being complete at *ca.* 900 K. Hydrogen consumption corresponds to a H_2/Fe ratio of 1.53 (expected value for complete reduction to Fe^0 1.50).[31] The broadness of the main peak makes it very difficult to perform a proper deconvolution analysis of this profile.

Finally, a TPR analysis of a Mg,Al-carbonate hydrotalcite gave rise to no hydrogen consumption, thus indicating that carbonate is evolved as CO_2 before being reduced to C (coke) or hydrocarbons.[29]

Therefore, it should be concluded that hydrogen consumption during TPR runs up to 1200 K will be exclusively due to reduction of cobalt and iron, and that both metals will be reduced to the zero-valent state.

The TPR profiles for the original samples are shown in Fig. 3. A single main reduction maximum is recorded at 656–693 K, reduction being complete at *ca.* 720 K, although minor reduction shoulders are also recorded for sample CoFeI (485 and 536 K) and for sample CoFeII (521 K). Bulk Co and Fe oxides are reduced at quite different temperatures (*ca.* 570 and 850 K, respectively), but in this case a single reduction step is recorded. It has been previously reported that reduction of two metals supported on the same support takes place simultaneously, despite the fact that they are reduced at different temperatures when present alone.[32] In our case, it can be tentatively assumed that hydrogen is dissociatively adsorbed on reduced Co particles, with further spillover of hydrogen atoms, thus lowering the reduction temperature of nearby iron oxide particles.

Although the starting cations were Co^{II} and Fe^{III}, a partial oxidation of Co^{II} to Co^{III} cannot be ruled out beforehand, if some similarity is expected between the samples here studied and the Co,Al-hydrotalcite-like material previously studied.[10] The $Co^{II} \rightarrow Co^{III}$ process is thermodynamically unfavoured in acidic conditions ($E^0_{Co^{3+}/Co^{2+}} = 1.82$ V at pH = 0),[33] but it is less unfavoured in a basic medium ($E^0_{Co(OH)_3/Co(OH)_2} = 0.17$ V at pH = 14). On the contrary, reduction of Fe^{3+} to Fe^{2+} is not expected. Therefore, hydrogen consumption during TPR runs would account for up to three different reduction processes:

$$Fe^{3+} \rightarrow Fe^0 \quad (3)$$

$$Co^{2+} \rightarrow Co^0 \quad (4)$$

$$Co^{3+} \rightarrow Co^0 \quad (5)$$

Experimental hydrogen consumptions were 13 370, 10 750 and 10 340 μmol H_2 (g solid)$^{-1}$, for samples CoFeI, CoFeH and CoFeII, respectively. From chemical analysis data included in Table 1, hydrogen consumptions to complete reactions (3) and (4), *i.e.*, assuming, in a first approximation, no $Co^{II} \rightarrow Co^{III}$ oxidation, would be 10 860, 10 670 and 9610 μmol H_2 (g solid)$^{-1}$, respectively, for these samples. The differences amount to 23, 0.7 and 7.6%, respectively. The difference for sample CoFeH is within experimental error, and so we should conclude that Co^{II} in this sample does not undergo any oxidation during synthesis. However, the values for samples CoFeI and CoFeII (especially the former) are large, and indicate

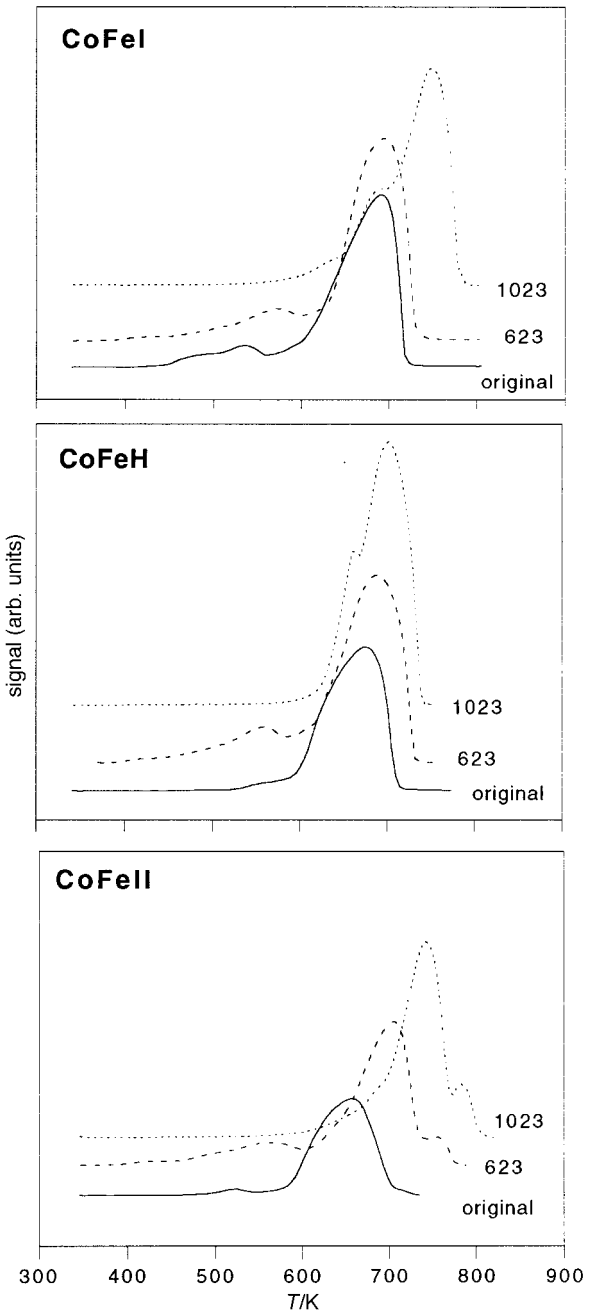

Fig. 3 Temperature-programmed reduction curves of original samples CoFeI, CoFeH and CoFeII, and after calcination at the temperatures given (in K)

that a partial oxidation of Co^{II} ions has taken place. Actually, the TPR profiles of these samples show weak hydrogen consumptions before the main reduction maximum. The question remains, however, how the oxidation process has taken place in samples maintained in air for several hours (at room temperature or at 343 K), a milder treatment than that used for sample CoFeH. It can be tentatively assumed that during hydrothermal treatment in a closed bomb the conditions were not as oxidizing as in the treatment in the oven in an open atmosphere. In the case of the Co,Al anionic clays previously studied,[10] oxidation was avoided by simply drying the sample in air for a few minutes.

Cobalt and iron are known as methanation catalysts, and so it could be also argued that the excess of hydrogen consumption (above the stoichiometric amount for Co^{II} and Fe^{III} reduction) corresponding to the reduction maxima before the main reduction maximum could be due to methane formation from interlayer carbonate. However, this possibility should

be ruled out, as reduction of these cations to the metallic state takes place at 656–693 K, *i.e.*, after these weak maxima; in other words, metallic phases do not exist in the temperature range where these weak maxima are recorded.

Study of the calcined samples

Calcination of layered double hydroxides leads to mixed oxides, the precise nature of which depends both on the composition of the parent LDH, the calcination temperature and the calcination time.[2,6,10,26] We have carried out a study of the species formed upon calcination of these three LDHs at 623 and 1023 K for 3 h in air. These calcination temperatures were chosen after the DTA study, which indicates (see Fig. 2) that the main thermal effects are recorded below 623 K; at 1023 K formation of well crystallized species is expected.

Taking into account the composition of a hydrotalcite-type material and that the M^{2+}/M^{3+} ratio should always be larger than unity,[2] calcination would lead to formation of spinel $M^{2+}M^{3+}{}_2O_4$, and the divalent cation in excess of the stoichiometric amount required to form the spinel would crystallize as its oxide, $M^{2+}O^{2-}$. However, the presence of oxidizable cations widens the range of species able to be formed.

The PXRD diagrams of the calcined samples are similar. Only peaks due to spinel phases are recorded. This is not surprising, taking into account that CoO (the rock-salt type single oxide expected to be formed without any oxidation process) is not stable at intermediate temperatures.[34] Those for sample CoFeII are shown in Fig. 4. In these samples, the following spinels can be formed: $Co^{II}Co^{III}{}_2O_4$, $Co^{II}Fe^{III}{}_2O_4$ and $Co^{II}Co^{III}Fe^{III}O_4$ as well as partial fractions of any of these species. PXRD patterns for Co_3O_4 and and $CoFe_2O_4$ are reported in JCPDS files (9-418 and 22-1086, respectively), but not that for Co_2FeO_4. The inset in Fig. 4 corresponds to the $55^\circ \leqslant 2\theta \leqslant 60^\circ$ range for sample CoFeII-623, where the maximum corresponding to planes (511) of spinels is recorded, and the tabulated positions for Co_3O_4 and $CoFe_2O_4$ are indicated. The position of the recorded maxima is within the values tabulated for these two spinels, but they do not coincide (a similar behaviour is observed for the other peaks). Probably, spinel Co_2FeO_4 (*i.e.*, $Co^{II}Co^{III}FeO_4$) exists in this sample calcined at 623 K. Taking into account the ionic radii of these cations,[35] when Fe^{III} substitutes for Co^{III} in Co_3O_4 to yield $Co^{II}Co^{III}FeO_4$, the spacings should be slightly larger (*i.e.*, diffraction maxima at lower 2θ values). Alternatively, if Co^{III} substitutes Fe^{III} in $CoFe_2O_4$ to yield $Co^{II}Co^{III}FeO_4$ the spacings should be slightly smaller (*i.e.*, diffraction maxima at larger 2θ values).

The analysis of the PXRD pattern for sample CoFeI-1023 is more complicated, as it cannot be ignored that a possible reaction of the spinels occurs at 623 K, resulting in transformation into other species, thus accounting for the larger number of peaks. However, it is noted that most of the seven rather broad peaks recorded for sample CoFeII-623 are split for sample CoFeII-1023. The low 2θ component of each doublet is always weaker than the high 2θ component, and the ratio between the intensities of these two components of the doublet is always constant. A notable behaviour, however, is the presence of a weak peak at 2.35–2.34 Å, without a counterpart. This peak was merely a shoulder of the most intense peak in the PXRD pattern of the sample calcined at 623 K. The weak peak corresponds to diffraction by planes (222) of the spinel, and its counterpart is included in the more intense peak due to planes (311).

If this splitting of the peaks is considered, the peaks now recorded are closer to those of $CoFe_2O_4$ (the component at lower 2θ within each doublet) and to those of Co_3O_4 (the component at higher 2θ value within each doublet), thus suggesting a reaction such as

$$\text{CoFe-LDH} \xrightarrow{623\ \text{K}} Co_2FeO_4 \xrightarrow{1023\ \text{K}} (1/3)\ CoFe_2O_4 + (2/3)\ Co_3O_4 \quad (6)$$

In order to investigate such reactions, sample CoFeII was submitted to calcination under two heating schemes: (i) by increasing the calcination time at 1023 K, and (ii) by increasing the calcination temperature for 3 h.

The PXRD diagrams of sample CoFeII calcined at 1023 K for 3, 24, 48 and 72 h in air are shown in Fig. 5. The splitting of the signals is clearly evident in all four samples. The positions of the maxima are always constant; so, the most intense peak is recorded at 2.458, 2.446, 2.446 and 2.451 Å, respectively, for the samples calcined for 3, 24, 48 and 72 h;

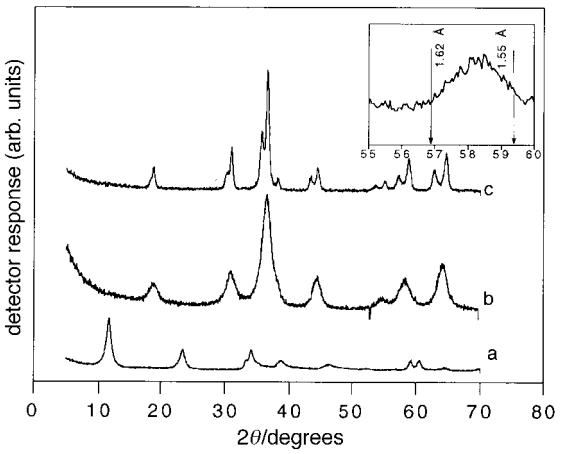

Fig. 4 Powder X-ray diffraction patterns of sample CoFeII: (a) original, and calcined in air 3 h at (b) 623 and (c) 1023 K. Inset: pattern for sample CoFeII calcined at 623 K for $55^\circ \leqslant 2\theta \leqslant 60^\circ$ (see text).

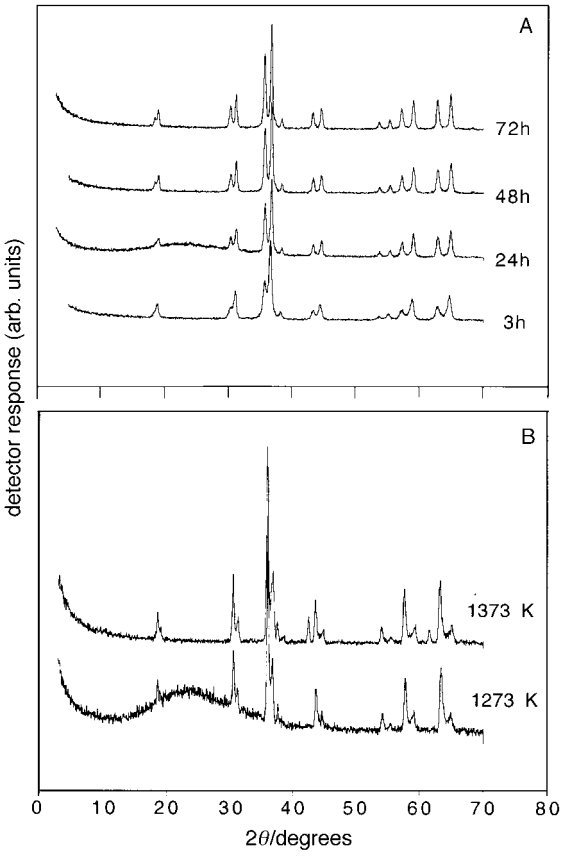

Fig. 5 Powder X-ray diffraction patterns of sample CoFeII calcined in air at 1023 K during the periods of time given (A), and for 3 h at the temperatures given (B)

the differences are very small and within experimental error. The only difference existing is the relative intensities between the two components of the doublet. For the most intense peak, due to planes (311), the intensity ratio (low 2θ component/high 2θ component) is 0.51, 0.70, 0.72 and 0.73, respectively, for samples calcined for 3, 24, 48 and 72 h. A small difference exists, but the ratio increases steadily with the calcination time.

A completely different behaviour is observed when the calcination temperature is increased to 1273 and 1373 K (the maximum reachable experimentally in our laboratory). The intensity of the high 2θ component sharply decreases when the calcination temperature is increased, and the peaks slightly shift, but without reaching the tabulated positions for $Co^{II}Fe^{III}{}_2O_4$ or Co_3O_4. For the sample calcined at 1373 K two new peaks develop at 2.127 and 1.505 Å, which coincide with the tabulated peaks for CoO. The other peak for CoO at 2.46 Å is probably obscured by the intense peaks of the spinel due to planes (311).

The decrease in the intensities of the high 2θ component of each doublet permits a clear detection of the peaks at 2.398 and 2.330 Å corresponding to planes (222) of the spinel; the first peak (2.398 Å) was not detected in the PXRD diagram of the sample calcined at 1023 K, as it is obscured by the intense peaks at 2.5 and 2.44 Å.

The evolution of the samples during calcination in air can be summarized as follows:

$$\text{CoFe-LDH} \xrightarrow{623\ \text{K}} Co^{II}Co^{III}{}_xFe^{III}{}_{2-x}O_4\ (x \approx 1) \qquad (7)$$

$$\text{CoFe-LDH} \xrightarrow{1023\ \text{K}} Co^{II}Co^{III}{}_yFe^{III}{}_{2-y}O_4 + Co^{II}Co^{III}{}_{2-z}Fe^{III}{}_zO_4\ (y \text{ and } z \text{ very small}) \qquad (8)$$

$$\text{CoFe-LDH} \xrightarrow{1373\ \text{K}} Co^{II}Co^{III}{}_yFe^{III}{}_{2-y}O_4 + Co^{II}Co^{III}{}_{2-z}Fe^{III}{}_zO_4 + CoO\ (y \text{ and } z \text{ very close to zero}) \qquad (9)$$

Calcination of the samples leads to important changes in their specific surface areas, with a value of $24 \pm 5\ m^2\ g^{-1}$ for samples calcined at 1023 K. Calcination leads to a degree of homogenization of the samples with regard to S_{BET} values, cancelling the differences observed for the parent samples. As with the non-calcined samples, the isotherms correspond to type II in the IUPAC classification, but with a narrow hysteresis loop for samples CoFeI-623 and CoFeII-623. Pore size distribution curves indicate a wide distribution for the samples calcined at 623 K, narrowing after calcination at 1023 K.

The FTIR spectra of the calcined samples are also very similar; the intensities of the bands at *ca.* 3400 and 1650 cm^{-1}, due to OH stretching and H_2O bending of water molecules (the hydroxy groups have been removed, according to the DTA–TG data) are very weak, and should correspond merely to physisorbed water molecules; removal of bands due to carbonate is also in agreement with the DTA–TG data. Sharp, intense bands develop at *ca.* 640 and 550 cm^{-1}, due to modes ν_1 and ν_2 of the spinel.

The TPR curves for the calcined samples are shown in Fig. 3, together with the profiles of the uncalcined materials. Unfortunately, the calcined samples could not be dissolved to carry out reliable chemical analyses, and so no quantitative analysis of the TPR profiles could be carried out. In all cases, calcination leads to a shift of the reduction maximum to higher temperatures. This behaviour is usually ascribed to an increase in the crystallinity of the samples, although formation of other amorphous or crystalline phases, as detected by PXRD, may also account for these differences. The main reduction maximum is recorded at 695 ± 10 K for the three samples calcined at 623 K, and weaker reduction peaks develop at temperatures (557–574 K) below that of the main maximum, suggesting a further formation of Co^{III} species in all three cases. These results are in agreement with the above PXRD data, showing formation of spinels, probably $Co^{II}Co^{III}Fe^{III}O_4$.

Calcination at 1023 K further shifts the main reduction maximum to higher temperatures, now being observed at 743–748 K for samples CoFeI and CoFeII, but at 703 K for sample CoFeH. The weak reduction maxima at 557–574 K have vanished, while a new maximum is recorded just below 700 K (693 K for sample CoFeI and 660 K for sample CoFeH), but it is almost absent for sample CoFeII, where a weak peak is recorded at 782 K. It should be remembered that the PXRD data discussed above showed that for samples calcined at 1023 K the spinel $Co^{II}Co^{III}Fe^{III}O_4$ is probably decomposing to $Co^{II}Co^{III}{}_2O_4$ and $Co^{II}Fe^{III}{}_2O_4$. The larger or lower amount of each of these species would be responsible for the different intensities and positions of these weak maxima around the main reduction peak.

Conclusions

The synthesis of $Co^{II}Fe^{III}$ hydrotalcites has been described. Depending on the experimental conditions, partial oxidation of Co^{II} to Co^{III} can be avoided. Reduction of these materials takes place in a single step (except reduction of Co^{III} species to Co^{II}, when the former were formed during synthesis), probably through reduction of Co^{II} and dissociative adsorption of hydrogen on the reduced particles, then being transferred by spillover to nearby Fe oxide particles, which are reduced at lower temperature than bulk Fe_2O_3. Decomposition in air leads to partial Co^{II} to Co^{III} oxidation, in the same temperature range as where decarbonation occurs.

Calcination at increasing temperatures gives rise to formation of spinels, segregating to better defined species at very high calcination temperatures, where CoO is formed in addition to other spinels.

The authors are grateful for financial support from Ministerio de Educación y Cultura (grant PB96–1307-C03–01) and Junta de Castilla y León (Consejería de Educación y Cultura, ref. SA45/96).

References

1 J. T. Richardson, *Principles of Catalyst Development*, Plenum Press, New York, 1989.
2 F. Cavani, F. Trifirò and A. Vaccari, *Catal. Today*, 1991, **11**, 1.
3 A. de Roy, C. Forano, K. El Malki and J. P. Besse, in *Expanded Clays and Other Microporous Solids*, ed. M. L. Occelli and H. E. Robson, Van Nostrand Reinhold, New York, 1992, p. 108.
4 F. Trifirò and A. Vaccari, in *Comprehensive Supramolecular Chemistry*, ed. J. L. Atwood, J. E. D. Davies, D. D. MacNicol, F. Vögtle, J.-M. Lehn, G. Alberti and T. Bein, Pergamon-Elsevier Science, Oxford, 1996, vol. 7, p. 251.
5 E. Uzunova, D. Klissurski and S. Kassabov, *J. Mater. Chem.*, 1994, **4**, 153.
6 E. Uzunova, D. Klissurski, I. Mitov and P. Stefanov, *Chem. Mater.*, 1993, **5**, 576.
7 K. Chibwe and W. Jones, *Chem. Mater.*, 1989, **1**, 489.
8 H. C. B. Hansen, C. B. Koch and R. M. Taylor, *J. Solid State Chem.*, 1994, **113**, 46.
9 F. Burriel, F. Lucena, S. Arribas and J. Hernández, *Química Analítica Cuantitativa*, 13th edn., Paraninfo, Madrid, 1989.
10 M. A. Ulibarri, J. M. Hernández, F. M. Labajos and V. Rives, *Chem. Mater.*, 1991, **3**, 626.
11 M. del Arco, M. V. G. Galiano, V. Rives, R.Trujillano and P. Malet, *Inorg. Chem.*, 1996, **35**, 6362.
12 V. Rives, *Adsorpt. Sci. Technol.*, 1991, **8**, 95.
13 P. Malet and A. Caballero, *J. Chem. Soc., Faraday Trans.*, 1988, **84**, 2369.

14 F. M. Labajos, V. Rives and M. A. Ulibarri, in *Multifunctional Mesoporous Inorganic Solids*, Nato ASI Series, ed. C. A. C. Sequeira and M. J. Hudson, Kluwer Academic, Dordrecht, 1993, vol. 400, p. 207.
15 A. S. Bookin and V. A. Drits, *Clays Clay Miner*., 1993, **41**, 551.
16 A. S. Bookin, V. I. Cherkashim and V. A. Drits, *Clays Clay Miner*., 1993, **41**, 558.
17 M. A. Ulibarri, F. M. Labajos, V. Rives, R. Trujillano, W. Kagunya and W. Jones, *Inorg. Chem*., 1994, **33**, 2592.
18 M. Chibwe, J. B. Valim and W. Jones, in *Multifunctional Mesoporous Inorganic Solids*, Nato ASI Series, ed. C. A. C. Sequeira and M. J. Hudson, Kluwer Academic, Dordrecht, 1993, vol. 400, p. 191.
19 E. C. Kruissink, L. L. Van Reijen and J. R. H. Ross, *J. Chem. Soc., Faraday Trans. 1*, 1981, **77**, 649.
20 F. M. Labajos, V. Rives and M. A. Ulibarri, *J. Mater. Sci*., 1992, **27**, 499.
21 K. Nakamoto, *Infrared and Raman Spectra of Inorganic and Coordination Compounds*, J. Wiley and Sons, New York, 4th edn., 1986.
22 K. S. W. Sing, D. H. Everett, R. A. W. Haul, L. Moscou, R. A. Pierotti, J. Rouquerol and T. Sieminiewska, *Pure Appl. Chem*., 1985, **57**, 603.
23 L. Pesic, S. Salipurovic, V. Markovic, D. Vucelic, W. Kagunya and W. Jones, *J. Mater. Chem*., 1992, **2**, 1069.
24 M. del Arco, V. Rives, R. Trujillano and P. Malet, *J. Mater. Chem*., 1996, **6**, 1419.
25 F. M. Labajos and V. Rives, *Inorg. Chem*., 1996, **35**, 5313.
26 C. Barriga, J. M. Fernández, M. A. Ulibarri, F. M. Labajos and V. Rives, *J. Solid State Chem*., 1996, **124**, 205.
27 P. Porta, R. Dragone, G. Fierro, M. Inversi and M. L. Jacono, *J. Chem. Soc., Faraday Trans*., 1992, **88**, 311.
28 *CRC Handbook of Chemistry and Physics*, ed. C. W. Robert, CRC Press, Boca Ratón, FL, 61st edn., 1980.
29 V. Rives, M. A. Ulibarri and A. Montero, *Appl. Clay Sci*., 1995, **10**, 83.
30 R. R. Rajaram and P. A. Sermon, *J. Chem. Soc., Faraday Trans. 1*, 1981, **81**, 2577; 2593.
31 D. Lazarov, V. Rives, R. Klissurska, I. Mitov and D. Klissurski, *Mater. Lett*., 1996, **27**, 129.
32 S. Kacimi and D. Duprez, *Stud. Surf. Sci. Catal*., 1991, **71**, 581.
33 B. Douglas, D. McDaniel and J. Alexander, *Concepts and Models of Inorganic Chemistry*, J. Wiley & Sons, New York, 3rd edn., 1993.
34 D. Nichols, in *Comprehensive Inorganic Chemistry*, ed. J. C. Bailar Jr., H. J. Emeleus, R. Nyholm and A. Trotman-Dickenson, Pergamon Press, Oxford, 1973, p. 1053.
35 J. E. Huheey, E. A. Keiter and R. L. Keiter, *Inorganic Chemistry, Principles of Stucture and Reactivity*, Harper Collins, New York, 4th edn., 1993.

Paper 7/05503J; *Received* 29*th July*, 1997